

Lattice BGK Simulation of Multipolar Vortex Formation

Gábor Házi^{1,*} and Gábor Tóth²

¹ *Theoretical Thermohydraulics Group, MTA KFKI Atomic Energy Research Institute, H-1525, Konkoly Th, 29-33, Budapest, Hungary*

² *Department of Physics and Chemistry, Széchenyi István University, H-9026, Egyetem Tér 1, Győr, Hungary*

Received 3 March 2010; Accepted (in revised version) 12 April 2010

Available online 13 July 2010

Abstract. Analytical and numerical studies have shown that multipolar vortices can emerge in two-dimensional flow due to azimuthal normal mode perturbations of shielded vortices. It has been found that mode 2 and 3 perturbations can lead to the formation of stable tripoles and quadrupoles, respectively, while higher order modes result in more complex unstable compound vortices. We have used the lattice Boltzmann method to simulate the effect of azimuthal perturbations on shielded vortices at moderate Reynolds numbers. We have found that azimuthal normal mode perturbations result in the formation of multipoles, which decay due to viscous dissipation. We could also observe that the outcome of such simulations is very sensitive to the displacement of perturbations above wavenumber-3 excitations, in spite of the significant viscosity we used.

AMS subject classifications: 65M10, 76D17, 78M99

Key words: Lattice Boltzmann method, shielded vortex, stability.

1 Introduction

Coherent structures can spontaneously emerge in two-dimensional turbulent flows and the understanding of their formation from small-scale noise might give some insight into turbulent transport. The simplest and most common form of such coherent structures is the monopolar vortex, which contains a single recirculating zone. It is sometimes surrounded by an oppositely-signed vorticity ring, which together with the core form a shielded vortex. Azimuthal normal mode perturbations of shielded vortices can lead to the development of exotic compound coherent structures, so called multipoles [1–4]. For example, stable tripole can emerge from a shielded vortex due

*Corresponding author.

Email: gah@aeki.kfki.hu (G. Házi), tooth@csoma.elte.hu (G. Tóth)

to the growth and saturation of an azimuthal normal mode with wavenumber-2. The tripole consists of a vortex core and two opposite-sign satellite vortices. Wavenumber-3 can result in the formation of a stable quadrupole with one core vortex bound to three satellites. Strong higher order azimuthal perturbations can lead to the formation of more complex compound structures, which were found to be unstable to infinitesimally small perturbations. Laboratory and numerical experiments are in good agreement with the above observations.

We have used the lattice Boltzmann method (LBM) to simulate the effect of azimuthal perturbations on shielded vortices. The objective of this paper is twofold. The first is to demonstrate that LBM is able to model vortex instabilities. The second is to show that high order multipoles can be formed by adding strong high order azimuthal perturbations to shielded vortices at moderate Reynolds numbers, although these structures are very sensitive to the form and displacement of the initial disturbances.

2 Lattice Boltzmann method

For the simulations presented in this paper we used the LBM with BGK (Bhatnagar-Gross-Krook) collision operator. This method proved to be adequate for many specific fluid dynamics problems involving vortex dynamics (see e.g., [5–7]). The method is based on the solution of the lattice Boltzmann equation (see [8] for further details)

$$f_i(\mathbf{x} + \mathbf{c}_{i\alpha}\delta, t + \delta) - f_i(\mathbf{x}, t) = -\frac{1}{\tau} [f_i(\mathbf{x}, t) - f_i^{eq}(\mathbf{x}, t)], \quad (2.1)$$

where f_i is the one particle velocity distribution function, $c_{i\alpha}$ is the discrete particle velocity, δ is the timestep, i is the index of the lattice links and the local equilibrium distribution function is given as follows

$$f_i^{eq} = \rho w_i \left(1 + \frac{u_\alpha c_{i\alpha}}{c_s^2} + \frac{u_\alpha u_\beta}{2c_s^4} Q_{i\alpha\beta} \right), \quad (2.2)$$

where

$$Q_{i\alpha\beta} = c_{i\alpha} c_{i\beta} - c_s^2 \delta_{\alpha\beta},$$

w_i is the lattice weight and c_s is the speed of sound. For the simulations presented in this paper, we used a D2Q9 model [9]. The macroscopic quantities are obtained from the distribution functions by taking their moments

$$\rho = \sum_i f_i, \quad \rho u_\alpha = \sum_i c_{i\alpha} f_i. \quad (2.3)$$

The pressure and the kinematic viscosity are given by

$$p = \rho c_s^2, \quad \nu = c_s^2 \left(\tau - \frac{1}{2} \right) \delta. \quad (2.4)$$

Recently, we have used the same model to study the interactions between shielded vortices [10].

3 Problem description and initial conditions

Simulation of the effect of azimuthal perturbations on shielded vortices have been carried out in a double-periodic box having a length L where $L = 2\pi$, placing a shielded Gaussian vortex at the centre of the domain. The initial vorticity profile was given as follows:

$$\omega(r) = -\omega_0 \left[\frac{1}{2} \alpha \left(\frac{r}{r_0} \right)^\alpha - 1 \right] e^{-(r/r_0)^\alpha}, \quad (3.1)$$

where $r = \sqrt{x^2 + y^2}$ and ω_0 is the initial vorticity in the centre. We define the Reynolds number based on the initial velocity maxima u_{\max} , vortex radius r_0 and kinematic viscosity ν , i.e., $Re = u_{\max} r_0 / \nu$. The time is non-dimensionalised by the initial turnover time calculated as follows $T = 2\pi^2 / \omega_0$. Vortex interactions due to periodicity has been avoided by a small ratio of vortex size to domain length: 0.065.

To excite azimuthal normal modes, the initial vorticity profile has been perturbed by adding the perturbation

$$\omega'(r, \theta) = \mu \left(\frac{r}{r_0} \right)^k \cos(k\theta) e^{-\left[\frac{\alpha(r/r_0)^\alpha - 2}{2\sigma} \right]^2}, \quad (3.2)$$

to the initial vorticity field. The amplitude and latitude of the perturbation can be controlled by the parameters μ and σ , respectively. Similar perturbations were applied e.g., in [3] without the multiplier $(r/r_0)^k$, what we have used to ensure that the vorticity distribution satisfies the pole condition at $r = 0$. In Fig. 1, some initial vortex profiles and perturbations are shown at various steepness and perturbation parameters ($\alpha = 2, 5, 7$, $\mu = 0.25, 0.5$ and $\sigma = 2, 10, 400$).

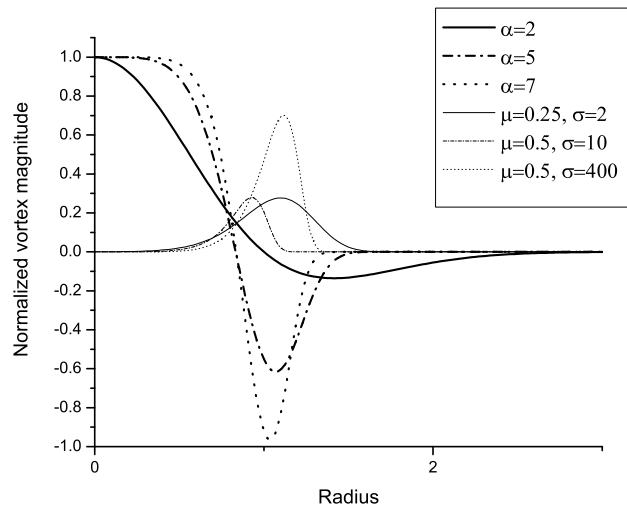


Figure 1: Initial vorticity profiles and perturbations (at $\theta = 0$) are shown for various α , μ and σ .

Knowing the initial vorticity field, one can solve the corresponding Poisson equation to obtain the streamfunction and then the velocity field can be derived. Assuming constant densities ($\rho = 1$) and knowing the initial velocity field we have initialized the particle distribution functions by their equilibrium values. Although there are more accurate and more sophisticated methods to initialize LBM, we have found that even this simple procedure can lead to accurate results as we demonstrate in the following section.

4 Numerical performance of LBM

In order to obtain information about the accuracy of LBM, we have studied the effect of azimuthal normal mode 3 perturbation on a shielded Gaussian vortex by LBM and compared the simulation results with solutions obtained by a pseudospectral solver. It is worth noting that there are more sophisticated approaches to simulate vortex dynamics (e.g., the contour dynamics method [11]) than the pseudospectral one for substantially higher Reynolds numbers than we used in the present study. However, for the current numerical experiments we focus on vortex stability in the viscous regime and here contour dynamics is not suitable and a direct comparison with pseudospectral computations suffices.

Our 2D Fourier pseudospectral approach solves the vorticity formulation of the 2D Navier-Stokes equations in double-periodic domain

$$\frac{\partial \omega}{\partial t} + u_\alpha \partial_\alpha \omega = \nu \partial_\alpha^2 \omega, \quad (4.1)$$

with 2/3 dealiasing scheme. The streamfunction is obtained by solving the Poisson equation

$$\partial_\alpha^2 \psi = -\omega, \quad (4.2)$$

and time integration is performed by a second-order Adams-Bashforth scheme. For the calculation presented in this paper, we used 256 Fourier modes in each direction.

The effect of normal mode 3 perturbation ($k = 3, \mu = 0.1, \sigma = 4$) on a shielded Gaussian having a steepness parameter $\alpha = 7$ can be followed in Fig. 2. Here we show the results obtained by LBM (top column) and by the pseudospectral approach (bottom column). The same contour levels are shown on both sides and each row represents the results at a time level ($T = 1, 2$ and 5). Solid lines represent positive vorticity and dotted lines are used for negative contours. In LBM we used the resolution 768^2 , which corresponds to the resolution of the spectral approach in the physical space. Obviously, the results agree very well with each other. Differences can be observed in the third line after the development of satellite vortices. Here some small deviations can be seen in the outermost contour lines, but the difference is quite negligible. Indeed, LBM is slightly more dissipative than the pseudospectral approach as it can be seen in Fig. 2, where the evolution of the normalized enstrophy and kinetic energy are shown. Here lines represent LBM results and symbols are used for the results of

the pseudospectral approach. One can see that LBM somewhat underestimates both the kinetic energy and enstrophy as the time goes, but the contour lines in Fig. 1 show that this discrepancy has negligible effect on the evolution.

5 Results

Several simulations have been carried out using LBM by varying the steepness parameter α , the amplitude and deviation of the perturbation μ, σ and exciting different azimuthal modes k . In each simulation the Reynolds number was 1000. It is worth

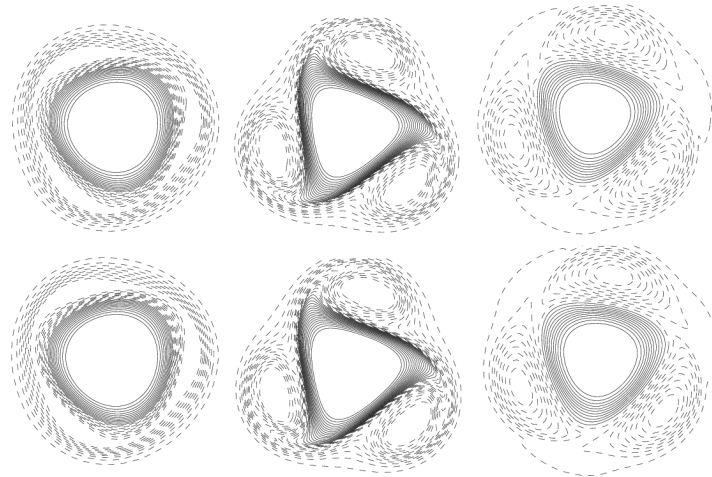


Figure 2: Contour lines are shown from the evolution in case of azimuthal normal mode perturbation 3 of a shielded vortex. The results obtained by LBM and by a pseudospectral method are shown on the top and bottom columns, respectively, at $T = 1, 2$ and 5). For more details see body text.

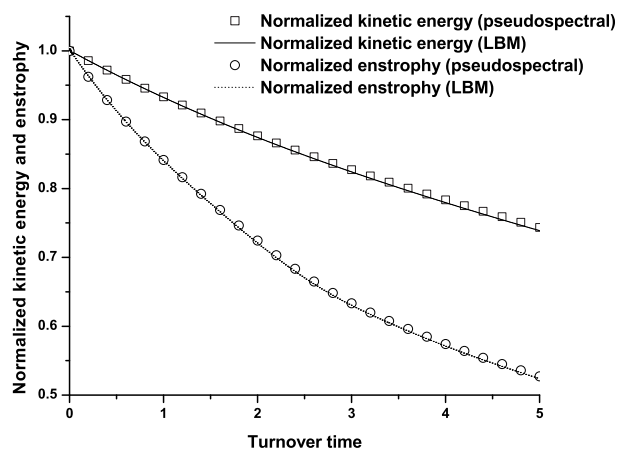


Figure 3: Evolution of the normalized kinetic energy and enstrophy in case of azimuthal normal mode perturbation 3 of a shielded vortex. Symbols represent the solution obtained by a pseudospectral method and solid/dashed lines are used to show the results of LBM.

noting again that in most of the earlier studies hyperviscosity was used to mimic "inviscid" flow in finite resolution simulations, while our aim was to study the problem in the viscous region. The results presented throughout the paper were obtained by using the resolution 768^2 . In effect, the perturbation can lead to three different scenarios in the viscous regime. The perturbation can die out without influencing the shape of the initial vortex profile, or it can result in a temporary multipolar vortex, which relaxes slowly to a shielded vortex. Or finally, the perturbation can cause the break of the initial vortex into dipolars. The outcome of the simulations depend on the parameters (k, μ, σ, α and Re). In this paper, we do not wish to study the whole parameter space spanned by these values. Rather we would like to show that increasing the wavenumber of the excitation there are some parameter sets, which yield the formation of quasi-stable multipolar vortex structures. To find such parameter sets, one can follow some simple rules: obviously k determines the pole number; σ must be sufficiently large to destroy a significant part of the shield, so its value is in relation with the steepness parameter α , which controls the wideness of the shield; μ must be sufficiently large to break the shield, but it must be small enough to avoid the break of the base vortex. Using these simple rules, one can easily find suitable parameters and varying further these values a regime map could be defined, but this is out of the scope of the present paper.

5.1 Formation of a tripole and dipolar breaking

Carton demonstrated that mode 2 perturbation ($k = 2$) of shielded vortices can lead to the formation of a tripole or it can cause dipolar breaking [1]. The outcome of such interactions depends on the strength of the perturbation and the steepness parameter. Although tripole is a rare object in nature and usually appears as the consequence of dipole collisions [12], its formation from an unstable monopole was first mentioned in [13], and later it has been observed both in laboratory [14] and numerical experiments [1, 12]. Furthermore tripoles appeared in more complex situations, too, e.g., in the ocean [15] or during the simulation of two-dimensional turbulence [16]. Orlandi and van Heijst [12], Beckers et al. [17], Flor and van Heijst [18] extended Carton's stability analysis considering shielded vortices and compared simulation results with laboratory observations. Most of these studies focused on the low viscosity region and there is only a few investigators, who studied the Reynolds number dependence of tripole formation, e.g., Rossi et al. [19] investigated the erosion of tripolar structures as the Reynolds number decreases.

In Fig. 4, one can see some stages of tripole formation as a result of azimuthal normal mode 2 perturbation of a shielded vortex, which has a steepness parameter $\alpha = 2$. The parameters of the perturbation are

$$\mu = 0.1, \quad \text{and} \quad \sigma^2 = 10.$$

Similar numerical simulations were carried out in [20] by a pseudospectral code with hyperviscosity and using different steepness parameter $\alpha = 3$. In spite of the dif-

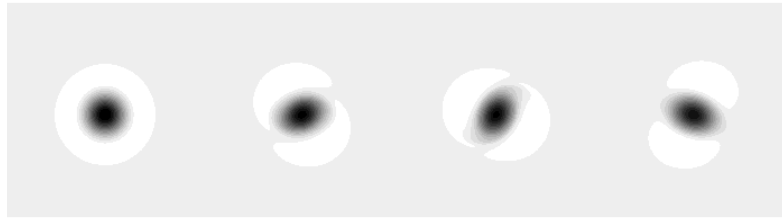


Figure 4: Formation of a tripole is shown by shaded contour plots of vorticity at $T = 0, 4, 5, 7$. Hereupon, uniform grey away from the central region indicates zero vorticity, black and darker grey indicate negative vorticity, white and lighter grey indicate positive vorticity. Parameters: $\alpha = 2, \sigma^2 = 10, \mu = 0.1$.

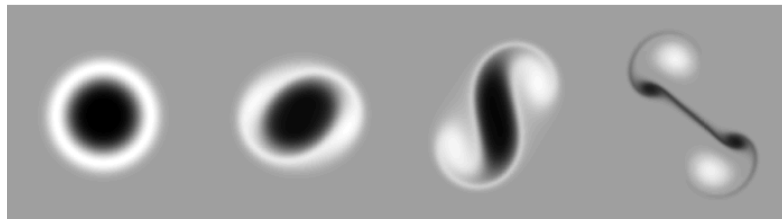


Figure 5: Stages of dipolar breaking is shown at $T = 0, 1, 3, 8$. Parameters: $\alpha = 5, \sigma^2 = 10, \mu = 0.5$.

ferences in the initial conditions and dissipation mechanism the evolution is pretty similar. The perturbation breaks the axisymmetry of the shield and the small vortex filaments erodate as the vortex rotates. After perfect breaking of the shield, two satellites develop which rotate together with the core and dissipate due to molecular diffusion. Not like in low viscosity simulations, here the satellites remain in touch with the vortex core. It is worth noting that the tripolar structure remains coherent after its formation in spite of the viscous dissipation.

The scenario is completely different when we increase both the steepness parameter and the magnitude of the perturbation. In Fig. 5, the evolution of an $\alpha = 5$ vortex is shown seeded by mode 2 perturbation having magnitude $\mu = 0.5$ and deviation $\sigma^2 = 10$. The first stage of this run is very similar to the former case. The vortex core takes an ellipsoid shape as a consequence of the perturbation. In the second stage the core becomes elongated and the satellites produce a shear which stretches the core until seceding. Finally the initial vortex breaks into two dipoles, which move away from each other. With the increase of the steepness parameter, the shield becomes thinner and the high amplitude perturbation, which has the same deviation (wideness) than before, can act not only on the shield but the core, too. As a consequence, the vortex breaks up and dipoles are formed.

5.2 Formation of a triangular vortex

The emergence and evolution of triangular vortices were studied in details by Carnevale and Kloosterziel [3] using numerical techniques and performing laboratory experiments. As it was first demonstrated by Carton [1] a triangular vor-

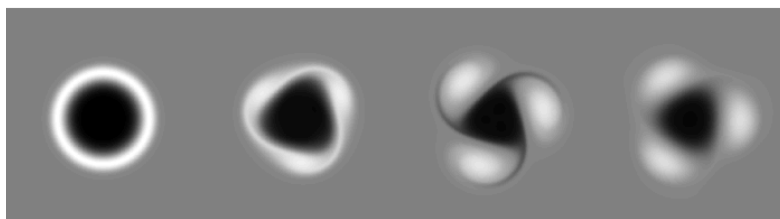


Figure 6: Formation of a triangular vortex is shown at $T = 0, 1, 4, 8$. Parameters: $\alpha = 7, \sigma^2 = 10, \mu = 0.1$.

tex (or quadrupole) can be formed by perturbing a shielded vortex with azimuthal wavenumber-3. In Fig. 6, we show the effect of such perturbation on an $\alpha = 7$ vortex. The parameters of the perturbation were $\mu = 0.1$ and $\sigma^2 = 10$. In the first stage there are three shrinking regions in the shield as a consequence of the perturbation. These regions then separate from each other and interact with the shield through three thin vortex filaments. As the filaments erode, the effect of perturbation saturates and a stable compound vortex forms having three satellites around an opposite-sign core. The satellites rotate around the center of the core and dissipate slowly due to molecular diffusion. The same observations were given by Carnevale and Kloosterziel [3] both in their laboratory experiments and numerical simulations. Studying Rankine vortices Morel and Carton [2] gave also similar observations. Carnevale and Kloosterziel [3] found that the triangular vortex is less robust than a tripole, but more stable than higher order structures. Therefore we performed a number of numerical experiments by using different displacements for the perturbation and moving it away from the axis of the initial vorticity profile. In the viscous region where we have worked we found that the triangular vortex is quite robust or at least it is much more robust than its higher order mates, which proved to be unstable for the smallest displacements we applied, see later on.

5.3 Formation of a square vortex

There were several attempts to produce square vortices by exciting azimuthal mode 4 in a shielded vortex. Most of such laboratory and numerical experiments failed to produce a stable structure (see Carnevale and Kloosterziel [3]). A square vortex formed by applying normal mode 4 perturbation, disintegrated very rapidly after its development demonstrating its sensitivity to small perturbations. In the viscous region the situation is similar. Although, we were able to produce a square vortex temporarily by adding azimuthal mode 4 perturbation to a shielded vortex, but we have found that the formation of such vortices is very sensitive both for the perturbation parameters and the displacement of the perturbations. Fig. 7 shows one case when we were succeeded. Here we perturbed an $\alpha = 5$ vortex with a perturbation using the parameters $\mu = 0.5$ and $\sigma^2 = 10$. The evolution is very similar to the former cases. Thinning of four regions in the shield (not shown here) lead to the formation of vorticity tentacles, which erode and leave four satellites around the core. At that time, the core takes a

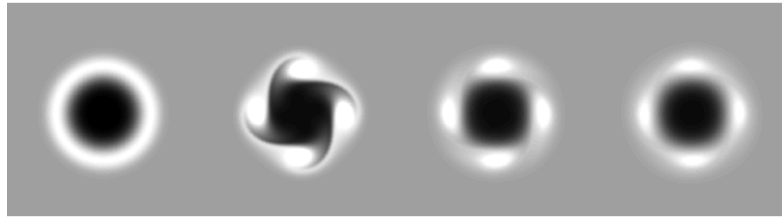


Figure 7: Formation of a square vortex is shown at $T = 0, 1, 3, 6$. Parameters: $\alpha = 5, \sigma^2 = 10, \mu = 0.5$.

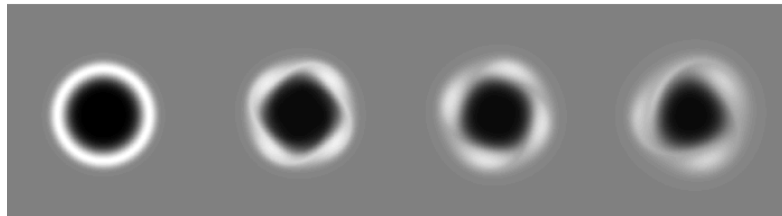


Figure 8: The effect of perturbation displacement is shown for a mode 4 excitation at $T = 0, 1, 4, 7$. Parameters: $\alpha = 7, \sigma^2 = 10, \mu = 0.1$.

square shape, which however, becomes more rounded as the evolution advances. It is worth noting that the four satellites emerge inside the shield which is not completely destroyed in this case.

How sensitive this structure to perturbation displacements can be demonstrated by shifting the axis of the perturbation with one lattice grid away from the axis of the initial $\alpha = 7$ vortex core. The parameters of the perturbations are $\mu = 0.1$ and $\sigma^2 = 10$ and the effect of the displacement can be followed in Fig. 8. Although initially a square vortex develops with four satellites, but later two of them merge due to the small asymmetry caused by the displacement. As they merge the core is also deformed and it takes a triangular shape. This shape is quite robust and keeps its structure for a while. Similar observations were given by Carnevale and Kloosterziel [3] studying the stability of a triangular vortex. They also observed the merging of two satellites of a triangular vortex and its metamorphosis to a kind of tripole, which finally broke into self-propelling dipolars.

5.4 Formation of high order coherent structures

Now, it might seem to be trivial that higher order azimuthal perturbations lead to more exotic coherent structures. Exciting mode $k = 5$, for instance, lead to the formation of a pentagon vortex (Fig. 9), while $k = 6$ gives a hexagon structure (Fig. 10). Although, in these simulations the satellites exceed only for a short time of period before melting into the shield, their more progressive development is only a question of the applied perturbation and steepness parameters. Here we used the parameters $\sigma^2 = 10$ and $\mu = 0.1$ and the steepness parameter was $\alpha = 5$. Since the development of these structures is very unlikely in nature, we did not make an attempt to find a

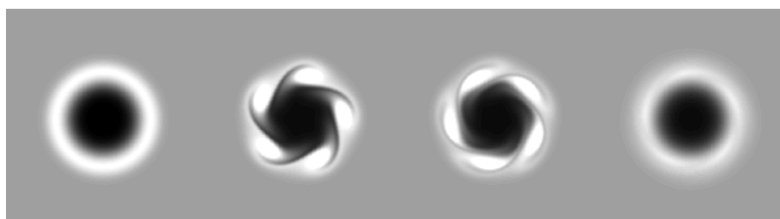


Figure 9: Formation of a pentagonal vortex is shown at $T = 0, 1, 2, 7$. Parameters: $\alpha = 5, \sigma^2 = 10, \mu = 0.1$.

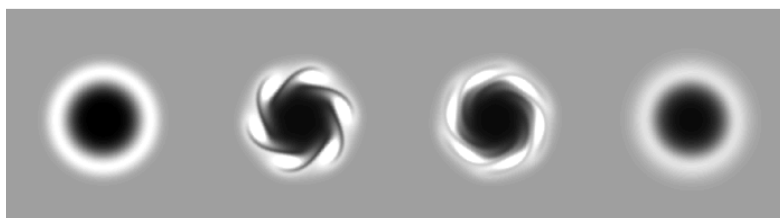


Figure 10: Formation of a hexagonal vortex is shown at $T = 0, 1, 2, 7$. Parameters: $\alpha = 5, \sigma^2 = 10, \mu = 0.1$.



Figure 11: Formation of vortex crystal is shown at $T = 0, 1, 2, 7$. Parameters: $\alpha = 5, \sigma^2 = 10, \mu = 0.5$.

perfect parameter set for more stringent demonstration.

We believe that it is much more interesting what happens with such high order structures when the perturbation is sufficiently large. Fig. 11 shows the evolution of an $\alpha = 5$ vortex when it is perturbed with a strong $k = 5$ mode ($\mu = 0.5$ and $\sigma^2 = 10$). The vortex breaks into dipoles, which rotate together with the core and form a kind of vortex crystal for a while. Such kind of vortex crystals were observed in [21] and their appearance were explained by approaching a maximum entropy state. Based on these simulation results another possible explanation will be given elsewhere.

6 Conclusions

We used the lattice Boltzmann method to simulate normal mode instabilities of shielded vortices. We demonstrated that the method is able to simulate the saturation of these modes and the formation of multipoles. Although we performed these simulations at moderate Reynolds numbers and used normal molecular diffusion mechanism, we found that the development of square or higher order vortices in nature is very unlikely, because these structures are very sensitive to normal mode displace-

ment. On the other hand strong azimuthal normal mode perturbation can lead to the development of vortex crystals which seem to be stable structures for a period of time.

Acknowledgments

This work was supported by the János Bolyai Research Scholarship of the Hungarian Academy of Sciences.

References

- [1] X. J. CARTON, *On the merger of shielded vortices*, Europhys. Lett., 18 (2002), pp. 697–703.
- [2] Y. G. MOREL AND X. J. CARTON, *Multipolar vortices in two-dimensional incompressible flows*, J. Fluid. Mech., 267 (1994), pp. 23–51.
- [3] G. F. CARNEVALE AND R. C. KLOOSTERZIEL, *Emergence and evolution of triangular vortices*, J. Fluid. Mech., 259 (1994), pp. 305–331.
- [4] X. CARTON AND B. LEGRAS, *The life-cycle of tripoles in two-dimensional incompressible flows*, J. Fluid. Mech., 267 (1994), pp. 53–82.
- [5] S. MENON AND J. H. SOO, *Simulation of vortex dynamics in three-dimensional synthetic and free jets using the large-eddy lattice Boltzmann method*, J. Turb., 5 (2004), N32.
- [6] S. K. BHAUMIK AND K. N. LAKSHMISHA, *Lattice Boltzmann simulation of lid-driven swirling flow in confined cylindrical cavity*, Comp. Fluids., 36 (2007), pp. 1163–1173.
- [7] M. CHENG, J. LOU AND T. T. LIM, *Motion of a vortex ring in a simple shear flow*, Phys. Fluids., 21 (2009), 081701.
- [8] S. CHEN AND G. D. DOOLEN, *Lattice Boltzmann method for fluid flows*, Ann. Rev. Fluid. Mech., 30 (1998), pp. 329–364.
- [9] Y. H. QIAN, D. D’HUMIÉRES AND P. LALLEMAND, *Lattice BGK models for Navier-Stokes equation*, Europhys. Lett., 17 (1992), pp. 479–484.
- [10] G. TÓTH AND G. HÁZI, *Merging of shielded Gaussian vortices and formation of a tripole at low Reynolds numbers*, accepted for publication in Phys. Fluids.
- [11] D. G. DRITSCHEL, *Contour dynamics and contour surgery: numerical algorithms for extended, high-resolution modelling of vortex dynamics in two-dimensional, inviscid, incompressible flow*, Comp. Phys. Rep., 10 (1989), pp. 77–146.
- [12] P. ORLANDI AND G. F. VAN HEIJST, *Numerical simulation of tripolar vortices in 2D flow*, Fluid. Dyn. Res., 9 (1992), pp. 179–206.
- [13] C. E. LEITH, *Minimum enstrophy vortices*, Phys. Fluids., 27 (1984), pp. 1388–1395.
- [14] G. J. F. VAN HEIJST AND R. C. KLOOSTERZEIL, *Tripolar vortices in a rotating fluid*, Nature., 338 (1989), pp. 569–571.
- [15] R. D. PINGREE AND B. LE CANN, *Three anticyclonic slope water ocean eddies (SWODDIES) in the southern Bay of Biscay in 1990*, Deep-Sea. Res., 39 (1992), pp. 1147–1175.
- [16] B. LEGRAS, P. SANTANGELO AND R. BENZI, *High-resolution numerical experiments for forced two-dimensional turbulence*, Europhys. Lett., 5 (1988), pp. 37–42.
- [17] M. BECKERS, H. J. H. CLERCX, G. J. F. VAN HEIJST AND R. VERZICCO, *Evolution and instability of monopolar vortices in a stratified fluid*, Phys. Fluids., 15 (2003), pp. 1033–1046.
- [18] J. B. FLÓR AND G. J. F. VAN HEIJST, *Stable and unstable monopolar vortices in a stratified fluid*, J. Fluid Mech., 311 (1996), pp. 257–287.

- [19] L. F. ROSSI, J. F. LINGEVITCH AND A. J. BERNOFF, *Quasi-steady monopole and tripole attractors for relaxing vortices*, Phys. Fluids, 9 (1997), pp. 2329–2338.
- [20] R. C. KLOOSTERZIEL AND G. F. CARNEVALE, *On the evolution and saturation of instabilities of two-dimensional isolated circular vortices*, J. Fluid. Mech., 388 (1999), pp. 217–257.
- [21] D. Z. JIN AND D. H. E. DUBIN, *Regional maximum entropy theory of vortex crystal formation*, Phys. Rev. Lett., 80 (1998), pp. 4434–4437.